EXTENSION OF SIGN-PERTURBED SUMS METHOD TO MULTIVARIATE SYSTEMS

Masanori Oshima [a], Sanghong Kim [b,*] , Yuri A. W. Shardt [c], Ken-Ichiro Sotowa [a]

[a] Department of Chemical Engineering, Kyoto University, Nishikyo-ku, Kyoto, 615-8510, Japan

[b] Department of Applied Physics and Chemical Engineering, Tokyo University of Agriculture and Technology, Naka-cho, Koganei-city, Tokyo 184-8588, Japan

[c] Department of Automation Engineering, Technical University of Ilmenau, P.O. Box 10 05 65, Ilmenau D-98684, Germany

Abstract

It is important to assess the accuracy of the dynamic model obtained by system identification before its implementation to a model-based control system. Especially in practical situations, it is required to use finite-sample data for the assessment of model accuracy, that is, asymptotic theory, which assumes infinite-sample data, cannot be used. The sign-perturbed sums (SPS) method can exactly assess the model accuracy using finite-sample, input-output data. SPS calculates the confidence region of the process parameters using resampled data sets that are obtained by sign-perturbation of the noise innovation. However, the application of the SPS method to multivariate processes has not been reported. In this paper, an extended SPS method that can handle multivariate processes is proposed. Moreover, it is shown by both a theoretical proof and a numerical example that the proposed method can calculate the exact confidence region. In the numerical example, the errors between the true and empirical confidence probabilities are smaller than 0.14%.

Keywords

Closed-loop identification, Confidence region, Finite-sample data.

Introduction

In model-based control systems, such as model predictive control systems, the accuracy of the dynamic model affects the control performance directly. Hence, it is important to evaluate the model accuracy before it is used for control, as well as to construct an accurate model. When the model accuracy turns out to be terrible, the resulting problems caused by the implementation of the model-based control can be prevented. In addition, evaluating model accuracy can provide clues to constructing an accurate model. For the above reasons, it is essential to determine the model accuracy exactly.

The models used for process control are often constructed using system identification (Darby and Nikolaou, 2012). Generally speaking, there are two types of system identification methods, open-loop identification and closed-loop identification. In open-loop identification, the process inputs are determined freely, and the identification result is likely to be accurate. However, a lot of time and effort are required to keep the production performance of the process during data acquisition. On the other hand, in closed-loop identification, the process inputs are determined by feedback controllers. Hence, closed-loop identification can save a lot of time and effort that are required in open-loop identification. However, model parameters obtained from closed-loop identification are likely to be biased because of the correlation between the manipulated variables and the output disturbances (Forssell and Ljung, 1999).

When comparing these two identification methods in the current situation, one is not always better than the other. However, closed-loop identification will be preferred in the future because the external situations of industrial plants will change more frequently. For example, the product demands will change faster as the idea of mass customization becomes more common, and the utility cost will also change faster as renewable energy, whose supply is unstable, becomes commonly used in plants. To handle such fast external changes, frequent update of the model is required. In such situations, closed-loop identification, which can work with past operating data accumulated in the plant, will be more suitable. Therefore, methods for assessing the model accuracy will be expected to handle not only open-loop identification but also

* Corresponding author. Email: sanghong@go.tuat.ac.jp.

closed-loop identification in the future.

Several studies have theoretically examined the accuracy of the model obtained from system identification (Soderstrom et al., 1976; Ljung, 1999; Wang et al., 2004; Bazanella et al., 2010; Shardt and Huang, 2011a,b; Yan et al., 2015). These studies derived the theoretical conditions where the modeling error converges to 0 as the number of samples goes to infinity. Therefore, while they are approximately true when the number of samples is large, the application of them to the case where a small number of samples are used may lead to wrong conclusions. Hence, it is necessary to correctly assess the accuracy of the model identified with finite-sample data.

Recently, several methods for assessing the accuracy of the model from system identification with finite-sample data were proposed by Weyer et al. (Csaji et al., 2015; Campi and Weyer, 2005; Care et al., 2018; Volpe et al., 2015). Using their methods, a confidence region, which includes the true process parameters with a given probability, can be calculated from the finite-sample data under the mild assumption that the noise innovation follows a symmetric distribution about 0.

Among their methods, only the sign-perturbed sums (SPS) method can be applied to closed-loop systems (Csaji and Weyer, 2015). However, the application of the SPS method to multivariate processes has not been discussed yet. Since the industrial plant has multiple input and output variables, it is required to extend SPS so that it can handle the data from multivariate processes. In this paper, the SPS method is extended to handle the finite-sample data obtained from multivariate processes.

Problem Setting

Figure 1 shows the process of interest. Let the true process be represented by an autoregressive exogenous (ARX), M-input, N-output linear system such as

$$\boldsymbol{y}(t) = \boldsymbol{G}(q^{-1})\boldsymbol{u}(t) + \boldsymbol{H}(q^{-1})\boldsymbol{e}(t), \tag{1}$$

$$\boldsymbol{G}(q^{-1}) = \begin{bmatrix} G_{1,1}(q^{-1}) & \cdots & G_{1,M}(q^{-1}) \\ \vdots & & \vdots \\ G_{N,1}(q^{-1}) & \cdots & G_{N,M}(q^{-1}) \end{bmatrix}, \tag{2}$$

$$\boldsymbol{H}(q^{-1}) = \begin{bmatrix} H_1(q^{-1}) & & 0 \\ & \ddots & \\ 0 & & H_N(q^{-1}) \end{bmatrix}, \tag{3}$$

where $\boldsymbol{u}(t) = [u_1(t), \cdots, u_M(t)]^\top \in \mathbb{R}^M$, $\boldsymbol{y}(t) = [y_1(t), \cdots, y_N(t)]^\top \in \mathbb{R}^N$, and $\boldsymbol{e}(t) = [e_1(t), \cdots, e_N(t)]^\top \in \mathbb{R}^N$ are the input, output and noise innovation vectors. Here, N and M can be different, that is, the extended SPS can be applied to nonsquare systems.

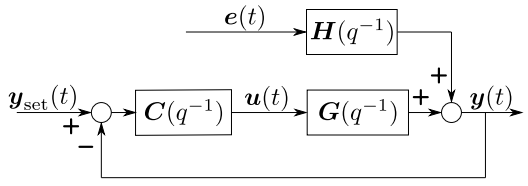

Figure 1: Control system considered in this paper.

For $\forall n \in \{1, 2, \cdots, N\}$ and $\forall m \in \{1, 2, \cdots, M\}$, $G_{n,m}(q^{-1})$ and $H_n(q^{-1})$ are rational functions of backward shift operator q^{-1} defined as

$$G_{n,m}(q^{-1}) = \frac{B_{n,m}(q^{-1})}{A_n(q^{-1})}, \tag{4}$$

$$H_n(q^{-1}) = \frac{1}{A_n(q^{-1})}, \tag{5}$$

$$A_n(q^{-1}) = 1 + a_{n,1}q^{-1} + \cdots + a_{n,K_n}q^{-K_n}, \tag{6}$$

$$B_{n,m}(q^{-1}) = b_{n,m,1}q^{-1} + \cdots + b_{n,m,L_{n,m}}q^{-L_{n,m}}, \tag{7}$$

where K_n and $L_{n,m}$ are non-negative integers. Based on Eqs. (1) to (7), the true process can be expressed as

$$\boldsymbol{y}(t) = \boldsymbol{\Phi}_0^\top(t)\boldsymbol{\theta}^* + \boldsymbol{e}(t). \tag{8}$$

The definitions of the regressor matrix $\boldsymbol{\Phi}_0(t) \in \mathbb{R}^{d \times N}$ and the true parameter vector $\boldsymbol{\theta}^* \in \mathbb{R}^d$ are

$$\boldsymbol{\Phi}_0(t) = \begin{bmatrix} \phi_{0,1}(t) & & & 0 \\ & \phi_{0,2}(t) & & \\ & & \ddots & \\ 0 & & & \phi_{0,N}(t) \end{bmatrix}, \tag{9}$$

$$\begin{aligned} \phi_{0,n}(t) = {} & [y_n(t-1), \cdots, y_n(t-K_n), \\ & u_1(t-1), \cdots, u_1(t-L_{n,1}), \\ & \cdots \\ & u_M(t-1), \cdots, u_M(t-L_{n,M})]^\top, \end{aligned} \tag{10}$$

$$\boldsymbol{\theta}^* = [\boldsymbol{\theta}_1^{*\top}, \boldsymbol{\theta}_2^{*\top}, \cdots, \boldsymbol{\theta}_N^{*\top}]^\top, \tag{11}$$

$$\begin{aligned} \boldsymbol{\theta}_n^* = {} & [a_{n,1}, \cdots, a_{n,K_n}, \\ & b_{n,1,1}, \cdots, b_{n,1,L_{n,1}}, \\ & \cdots \\ & b_{n,M,1}, \cdots, b_{n,M,L_{n,M}}]^\top, \end{aligned} \tag{12}$$

where d is the number of parameters included in the system and is calculated by

$$d = \sum_{n=1}^{N} \left(K_n + \sum_{m=1}^{M} L_{n,m} \right). \tag{13}$$

In the case of open-loop systems, $\boldsymbol{u}(t)$ is determined freely. On the other hand, when considering closed-loop systems, $\boldsymbol{u}(t)$ is calculated by

$$\boldsymbol{u}(t) = \boldsymbol{C}(q^{-1})(\boldsymbol{y}_{\mathrm{set}}(t) - \boldsymbol{y}(t)), \tag{14}$$

$$\boldsymbol{C}(q^{-1}) = \begin{bmatrix} C_{1,1}(q^{-1}) & \cdots & C_{1,N}(q^{-1}) \\ \vdots & & \vdots \\ C_{M,1}(q^{-1}) & \cdots & C_{M,N}(q^{-1}) \end{bmatrix}, \tag{15}$$

where $\boldsymbol{y}_{\mathrm{set}}(t) = [y_{\mathrm{set},1}(t), \cdots, y_{\mathrm{set},N}(t)]^\top \in \mathbb{R}^N$ is the setpoint vector, and $C_{m,n}(q^{-1})$ are the linear controllers. Note that $\{y_{\mathrm{set},n}\}_{t=1}^T$ can be an arbitrary, bounded signal.

Method

SPS calculates an exact confidence region of model parameters using time-series data with finite samples. The confidence region is a region defined in the parameter space where the true parameter vector $\boldsymbol{\theta}^*$ is included with probability p. When the value of p is fixed, the size of the confidence

region indicates the model accuracy, that is, the model accuracy increases as the size of the confidence region decreases. This means that SPS enables us to assess model accuracy using finite-sample data.

The basic idea of multivariate SPS is almost the same as SPS for single-input, single-output systems (Csaji et al., 2015). Multivariate SPS calculates the confidence region $D_{\mathrm{SPS}}(p) \subseteq \mathbb{R}^d$ by determining whether each parameter vector in $\mathbb{R}^d$ is included in the $D_{\mathrm{SPS}}(p)$. Let one of the considered parameter vectors be $\boldsymbol{\theta} \in \mathbb{R}^d$. Then, multivariate SPS resamples data sets by perturbing the signs of the estimate $\boldsymbol{\epsilon}_0(t,\boldsymbol{\theta}) = [\varepsilon_{0,1}(t,\boldsymbol{\theta}),\cdots,\varepsilon_{0,N}(t,\boldsymbol{\theta})]^\top \in \mathbb{R}^N$ of $\boldsymbol{e}(t)$, which is calculated by

$$\boldsymbol{\epsilon}_0(t,\boldsymbol{\theta}) = \boldsymbol{y}(t) - \boldsymbol{\Phi}_0^\top(t)\boldsymbol{\theta},\ \boldsymbol{y}(t),\boldsymbol{u}(t) \in \mathbb{D}_0, \tag{16}$$

where $\mathbb{D}_0 = \{\boldsymbol{y}(t),\boldsymbol{u}(t) \mid t = 1\cdots,T\}$, and $T \in \mathbb{N}$ is the number of samples.

The sign perturbation of $\boldsymbol{\epsilon}_0(t,\boldsymbol{\theta})$ is performed by multiplying $(R-1)N$ independent and identically distributed (i.i.d.) random sign $\{\alpha_{r,n}(t)\}_{t=1}^T$ $(r = 1,\cdots,R-1,\ n = 1,\cdots,N)$ to each element of $\boldsymbol{\epsilon}_0(t,\boldsymbol{\theta})$. Here, $\alpha_{r,n}(t)$ takes the values $+1$ and -1 with a probability of 0.5 each. The sign-perturbed noise innovation estimate $\boldsymbol{\epsilon}_r(t,\boldsymbol{\theta})\,(r = 1,\cdots,R-1)$ is given as

$$\boldsymbol{\epsilon}_r(t,\boldsymbol{\theta}) = [\alpha_{r,1}(t)\varepsilon_{0,1}(t,\boldsymbol{\theta}),\cdots,\alpha_{r,N}(t)\varepsilon_{0,N}(t,\boldsymbol{\theta})]^\top. \tag{17}$$

Using $\boldsymbol{\epsilon}_r(t,\boldsymbol{\theta})\,(r = 1,\cdots,R-1)$ as the noise innovation vectors, simulations for acquiring $(R-1)$ time-series data sets, $\mathbb{D}_r(\boldsymbol{\theta}) = \{\boldsymbol{y}_r(t,\boldsymbol{\theta}),\boldsymbol{u}_r(t,\boldsymbol{\theta}) \mid t = 1,\cdots,T\}\,(r = 1,\cdots,R-1)$, is performed. Here, $\boldsymbol{u}_r(t,\boldsymbol{\theta}) = [u_{r,1}(t,\boldsymbol{\theta}),\cdots,u_{r,M}(t,\boldsymbol{\theta})]^\top \in \mathbb{R}^M$ and $\boldsymbol{y}_r(t,\boldsymbol{\theta}) = [y_{r,1}(t,\boldsymbol{\theta}),\cdots,y_{r,N}(t,\boldsymbol{\theta})]^\top \in \mathbb{R}^N$ are the resampled input and output vectors.

Using $\mathbb{D}_0$ and $\mathbb{D}_r(\boldsymbol{\theta})\,(r = 1,\cdots,R-1)$, multivariate SPS calculates the *reference sum* $\boldsymbol{S}_0(\boldsymbol{\theta})$ and the *sign-perturbed sums* $\{\boldsymbol{S}_r(\boldsymbol{\theta})\}_{r=1}^{R-1}$ defined as

$$\boldsymbol{S}_\rho(\boldsymbol{\theta}) = \left(\frac{1}{T}\sum_{t=1}^T \boldsymbol{\Phi}_\rho(t)\boldsymbol{\Phi}_\rho^\top(t)\right)^{-\frac{1}{2}} \frac{1}{T}\sum_{t=1}^T \boldsymbol{\Phi}_\rho(t)\boldsymbol{\epsilon}_\rho(t,\boldsymbol{\theta}), \tag{18}$$
$$\rho = 0,1,\cdots,R-1,$$

where $\boldsymbol{\Phi}_r(t)\,(r = 1,\cdots,R-1)$ is

$$\boldsymbol{\Phi}_r(t) = \begin{bmatrix} \phi_{r,1}(t) & & 0 \\ & \phi_{r,2}(t) & \\ & & \ddots \\ 0 & & \phi_{r,N}(t) \end{bmatrix}, \tag{19}$$

$$\begin{aligned} \phi_{r,n} \quad = \quad & [y_{r,n}(t-1),\cdots,y_{r,n}(t-K_n), \\ & u_{r,1}(t-1),\cdots,u_{r,1}^\top(t-L_{n,1}), \\ & \cdots \\ & u_{r,M}(t-1),\cdots,u_{r,M}^\top(t-L_{n,M})]^\top. \end{aligned} \tag{20}$$

Multivariate SPS determines if $\boldsymbol{\theta}$ is included in $D_{\mathrm{SPS}}(p)$ by exploiting the fact that $\{||\boldsymbol{S}_\rho(\boldsymbol{\theta}^*)||\}_{\rho=0}^{R-1}$ is *uniformly ordered* with respect to (w.r.t.) $\prec_\pi$. Here, $\prec_\pi$ is a strictly total order defined for I real numbers $\{Z_i\}_{i=1}^I$ as

$$Z_k \prec_\pi Z_j \tag{21}$$

if and only if

$$(Z_k < Z_j) \text{ or } (Z_k = Z_j \text{ and } \pi(k) < \pi(j)), \tag{22}$$

where π is a bijection map from $\{1,2,\cdots,I\}$ to itself. In addition, "*uniformly ordered*" is defined in Definition 1.

Definition 1. *Let Z_1, $\cdots$, Z_I be random variables and $\prec$ be a strict total order. Then, $\{Z_i\}_{i=1}^I$ is uniformly ordered w.r.t. $\prec$ if and only if*

$$P(Z_{i_1} \prec Z_{i_2} \prec \cdots \prec Z_{i_I}) = \frac{1}{I!} \tag{23}$$

holds for any permutation $\forall\{i_1,i_2,\cdots,i_I\}$ of $\{1,2,\cdots,I\}$, where $P(\cdot)$ is the probability that the input event occurs.

Detailed procedure

In multivariate SPS, the following assumptions are made:

A.1 Each $\{e_n(t)\}_{t=1}^T$ is independent and follows a probability density function (PDF) symmetric about 0.

A.2 If $n_1 \neq n_2$, then $\{e_{n_1}(t)\}_{t=1}^T$ and $\{e_{n_2}(t)\}_{t=1}^T$ are independent of each other.

A.3 The matrices $\{\boldsymbol{R}_\rho\}_{\rho=0}^{R-1}$ defined as

$$\boldsymbol{R}_\rho = \frac{1}{T}\sum_{t=1}^T \boldsymbol{\Phi}_\rho(t)\boldsymbol{\Phi}_\rho^\top(t) \tag{24}$$

are invertible. In addition, Eq. (24) is equivalent to

$$\boldsymbol{R}_\rho = \begin{bmatrix} \boldsymbol{R}_{\rho,1} & & 0 \\ & \ddots & \\ 0 & & \boldsymbol{R}_{\rho,N} \end{bmatrix}, \tag{25}$$

where $\boldsymbol{R}_{\rho,n} = \frac{1}{T}\sum_{t=1}^T \boldsymbol{\phi}_{\rho,n}(t)\boldsymbol{\phi}_{\rho,n}^\top(t)$. Therefore, $\boldsymbol{R}_\rho$ is invertible if and only if $\boldsymbol{R}_{\rho,1}$, $\cdots$, $\boldsymbol{R}_{\rho,N}$ are invertible, and the inverse of $\boldsymbol{R}_\rho$ is given as

$$\boldsymbol{R}_\rho^{-1} = \begin{bmatrix} \boldsymbol{R}_{\rho,1}^{-1} & & 0 \\ & \ddots & \\ 0 & & \boldsymbol{R}_{\rho,N}^{-1} \end{bmatrix}. \tag{26}$$

A.4 The true process is included in the model set.

A.5 The external signals, $\{u_1(t)\}_{t=1}^T,\cdots,\{u_M(t)\}_{t=1}^T$ in the case of open-loop systems or $\{y_{\mathrm{set},1}(t)\}_{t=1}^T,\cdots\{y_{\mathrm{set},N}(t)\}_{t=1}^T$ in the case of closed-loop systems, are independent of $\{e_1(t)\}_{t=1}^T$, $\cdots$, $\{e_N(t)\}_{t=1}^T$.

Since A.1 does not require a particular kind of PDF of $\boldsymbol{e}(t)$, A.1 is likely to hold in many cases including practical ones, where the PDF of the noise innovation is usually unknown.

Under assumptions A.1 to A.5, the procedure for multivariate SPS is:

M.1 Determine $R \in \{2,3,\cdots\}$ and $\tilde{R} \in \{1,2,\cdots,R\}$, then the confidence probability is $p = 1-\tilde{R}/R$.

M.2 Generate $(R-1)$ sets of a random-sign time series $\{\alpha_r(t)\}_{t=1}^{T}\,(r=1,2,\cdots,R-1)$.

M.3 Determine $D_{\mathrm{SPS}}(p)$ according to the following equation:

$$D_{\mathrm{SPS}}(p) = \left\{ \boldsymbol{\theta} \in \mathbb{R}^d \mid I_{\mathrm{SPS}}(\boldsymbol{\theta}) = 1 \right\}. \tag{27}$$

Here, the definition of $I_{\mathrm{SPS}}(\cdot)$ is

$$I_{\mathrm{SPS}}(\boldsymbol{\theta}) = \begin{cases} 1 & (\text{if } \mathit{Rank}(\boldsymbol{\theta}) \le R-\tilde{R}), \\ 0 & (\text{otherwise}), \end{cases} \tag{28}$$

where $\mathit{Rank}(\boldsymbol{\theta})$ is defined as follows:

M.3.1 Calculate $\{\boldsymbol{\epsilon}_0(t,\boldsymbol{\theta})\}_{t=1}^{T}$ by Eq. (16)

M.3.2 Calculate $\{\boldsymbol{\epsilon}_r(t,\boldsymbol{\theta})\}_{t=1}^{T}\,(r=1,\cdots,R-1)$ by Eq. (17)

M.3.3 Aquire $\mathbb{D}_r(\boldsymbol{\theta})\,(r=1,\cdots,R-1)$ from the simulation of the system with $\boldsymbol{\theta}$ driven by $\{\boldsymbol{\epsilon}_r(t,\boldsymbol{\theta})\}_{t=1}^{T}\,(r=1,\cdots,R-1)$.

M.3.4 Calculate $\{\boldsymbol{S}_\rho(\boldsymbol{\theta})\}_{\rho=0}^{R-1}$ using Eq. (18).

M.3.5 Arrange $\{||\boldsymbol{S}_\rho(\boldsymbol{\theta})||\}_{\rho=0}^{R-1}$ from smallest to largest according to $\prec_\pi$, that is, $||\boldsymbol{S}_{\rho_1}(\boldsymbol{\theta})|| \prec_\pi ||\boldsymbol{S}_{\rho_2}(\boldsymbol{\theta})|| \prec_\pi \cdots \prec_\pi ||\boldsymbol{S}_{\rho_R}(\boldsymbol{\theta})||$, where $\{\rho_1,\cdots,\rho_R\}$ is a permutation of $\{0,1,\cdots,R-1\}$.

M.3.6 Define $\mathit{Rank}(\boldsymbol{\theta})$ as

$$\mathit{Rank}(\boldsymbol{\theta}) = i, \text{ if } ||\boldsymbol{S}_0(\boldsymbol{\theta})|| = ||\boldsymbol{S}_{\rho_i}(\boldsymbol{\theta})||. \tag{29}$$

When considering the open-loop systems, the data acquisition in Step M.3.3 is performed by

$$\boldsymbol{y}_r(t,\boldsymbol{\theta}) = \hat{\boldsymbol{G}}(q^{-1},\boldsymbol{\theta})\boldsymbol{u}(t) + \hat{\boldsymbol{H}}(q^{-1},\boldsymbol{\theta})\boldsymbol{\epsilon}_r(t,\boldsymbol{\theta}), \tag{30}$$

$$\boldsymbol{u}_r(t,\boldsymbol{\theta}) = \boldsymbol{u}(t), \tag{31}$$

where $\hat{\boldsymbol{G}}(q^{-1},\boldsymbol{\theta})$ and $\hat{\boldsymbol{H}}(q^{-1},\boldsymbol{\theta})$ are the transfer function matrices of the models of the process and the noise filter. In the case of closed-loop systems, on the other hand, the data acquisition in Step M.3.3 is performed using the closed-loop system described as

$$\boldsymbol{y}_r(t,\boldsymbol{\theta}) = \hat{\boldsymbol{G}}(q^{-1},\boldsymbol{\theta})\boldsymbol{u}_r(t,\boldsymbol{\theta}) + \hat{\boldsymbol{H}}(q^{-1},\boldsymbol{\theta})\boldsymbol{\epsilon}_r(t,\boldsymbol{\theta}), \tag{32}$$

$$\boldsymbol{u}_r(t,\boldsymbol{\theta}) = \boldsymbol{C}(q^{-1})(\boldsymbol{y}_{\mathrm{set}}(t) - \boldsymbol{y}_r(t,\boldsymbol{\theta})). \tag{33}$$

Theoretical background

$D_{\mathrm{SPS}}(p)$ includes the true process parameter $\boldsymbol{\theta}^*$ exactly with the probability p regardless of the quality of $\mathbb{D}_0$ and the value of R.

Theorem 2. *If assumptions A.1 to A.5 hold, for* $\forall R \in \{2,3,\cdots\}$ *and* $\forall \tilde{R} \in \{1,2,\cdots,R\}$*, the confidence probability of the confidence region obtained using the multivariate SPS method is exactly* $1-\tilde{R}/R$.

Proof. See appendix "**Proof of Theorem 2**". □

This property is mainly attributed to A.1. If $\boldsymbol{\theta} = \boldsymbol{\theta}^*$, then $\boldsymbol{\epsilon}_0(t,\boldsymbol{\theta}^*) = \boldsymbol{e}(t)$ from Eqs. (8) and (16). Because of this, the sign-perturbation of each element of $\boldsymbol{\epsilon}_0(t,\boldsymbol{\theta}^*)$ does not change the PDF from A.1, that is, $\{\boldsymbol{\epsilon}_\rho(t,\boldsymbol{\theta}^*)\}_{t=1}^{T}\,(\rho=0,\cdots,R-1)$ follows the same PDF. As a result, $\{||\boldsymbol{S}_\rho(\boldsymbol{\theta}^*)||\}_{\rho=0}^{R-1}$ are *uniformly ordered* w.r.t. $\prec_\pi$, and the probability that $||\boldsymbol{S}_0(\boldsymbol{\theta}^*)||$ is the ρ'-th smallest is $1/R$ for $\forall\rho' \in \{1,2,\cdots,R\}$. Therefore, the probability of $\mathit{Rank}(\boldsymbol{\theta}^*) \le R-\tilde{R}$, which corresponds to the probability that $\boldsymbol{\theta}^*$ is determined to be in the confidence region by multivariate SPS, is exactly $1-\tilde{R}/R$.

Numerical Example

In this section, the validity of the multivariate SPS method is confirmed through a numerical example of a 2-by-2 ARX process. Let the ARX process of interest be defined as:

$$\boldsymbol{G}(q^{-1}) = \begin{bmatrix} \dfrac{3.2q^{-1}}{1-0.6q^{-1}} & \dfrac{1.9q^{-1}}{1-0.6q^{-1}} \\ \dfrac{2.3q^{-1}}{1-0.8q^{-1}} & \dfrac{2.8q^{-1}}{1-0.8q^{-1}} \end{bmatrix}, \tag{34}$$

$$\boldsymbol{H}(q^{-1}) = \begin{bmatrix} \dfrac{1}{1-0.6q^{-1}} & 0 \\ 0 & \dfrac{1}{1-0.8q^{-1}} \end{bmatrix}, \tag{35}$$

where the sampling interval is 1 s. This ARX process is controlled by 2 proportional-integral (PI) controllers. Here, $y_1(t)$ and $y_2(t)$ are controlled by manipulating $u_1(t)$ and $u_2(t)$, respectively. The transfer function matrix of the controller is described as

$$\boldsymbol{C}(q^{-1}) = \begin{bmatrix} 1.75 + \dfrac{3.51q^{-1}}{1-q^{-1}} & 0 \\ 0 & 1.01 + \dfrac{2.02q^{-1}}{1-q^{-1}} \end{bmatrix} \times 10^{-3}. \tag{36}$$

Each element $y_{\mathrm{set},n}\,(n=1,2)$ of the setpoint vector is changed from 0 to 5 at $t=1$ s, that is,

$$y_{\mathrm{set},n}(t) = \begin{cases} 0, & t \le 1 \\ 5, & t > 1 \end{cases}, \; n = 1,2. \tag{37}$$

Each element $e_n\,(n=1,2)$ of the noise innovation vector is white noise with a Gaussian distribution whose mean and variance are, respectively, 0 and 0.1, that is,

$$e_n(t) \sim \mathcal{N}(0,0.1),\; n=1,2. \tag{38}$$

Note that assumption A.1 holds for the noise innovation defined as Eq. (38). In addition, the number of samples T of the time-series data is set to 200.

Calculation of the empirical confidence probability

In this subsection, it is confirmed that the proposed method can yield the exact confidence region by calculating empirical confidence probabilities p_{e} for several given confidence probabilities p. To calculate p_e, $I_{\mathrm{SPS}}(\boldsymbol{\theta}^*)$ is calculated 100,000 times for different seeds to generate $\{\boldsymbol{e}(t)\}_{t=1}^{T}$. Then, p_{e} is calculated as the mean of 100,000 simulations of $I_{\mathrm{SPS}}(\boldsymbol{\theta}^*)$.

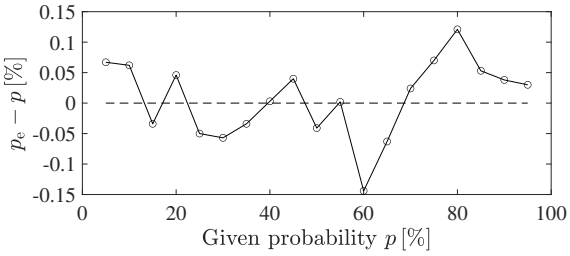

Figure 2: Errors $p_e - p$ between empirical and given confidence probabilities for several given confidence probability p.

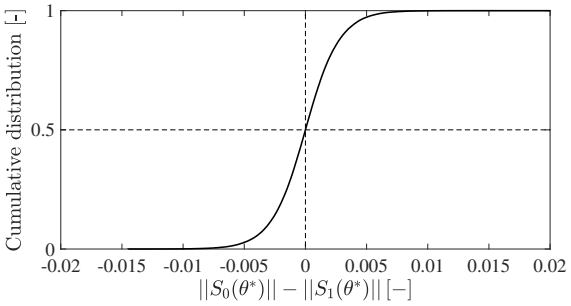

Figure 3: Cumulative distributions of the difference between the norms of reference and sign-perturbed sums at $\boldsymbol{\theta} = \boldsymbol{\theta}^*$.

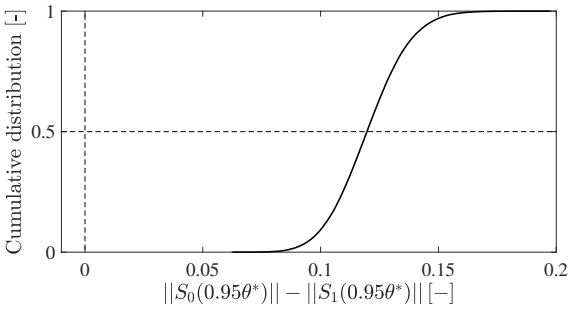

Figure 4: Cumulative distributions of the difference between the norm of reference and sign-perturbed sums at $\boldsymbol{\theta} = 0.95\boldsymbol{\theta}^*$.

The corresponding p_e to $p = 0.05, 0.10, \cdots, 0.95$ was calculated using the above procedure. Here, R is fixed at 100, and $\tilde{R}$ is changed to adjust p. The error between p and p_e is shown in Figure 2. From Figure 2, the maximum absolute error between p_e and p is 0.14%. Hence, the proposed extension of SPS can calculate the exact confidence region with a given p.

Change in a difference between reference and sign-perturbed sums against parameter error

Multivariate SPS determines if a given parameter vector $\boldsymbol{\theta}$ is included in $D_{\mathrm{SPS}}(p)$, based on the fact that $\{||\boldsymbol{S}_\rho(\boldsymbol{\theta}^*)||\}_{\rho=0}^{R-1}$ are *uniformly ordered* w.r.t. $\prec_\pi$. This means that the probability that the norm of *reference sum* is larger than one of the norms of *sign-perturbed sums* is exactly 0.5. In this subsection, this property is confirmed by drawing the cumulative distribution of the difference between $||\boldsymbol{S}_0(\boldsymbol{\theta})||$ and $||\boldsymbol{S}_1(\boldsymbol{\theta})||$.

For the 2 kinds of parameters, $\boldsymbol{\theta} = \boldsymbol{\theta}^*$ and $0.95\boldsymbol{\theta}^*$, $||\boldsymbol{S}_0(\boldsymbol{\theta})||$ and $||\boldsymbol{S}_1(\boldsymbol{\theta})||$ are calculated 100,000 times with different seed values to generate $\{\boldsymbol{e}(t)\}_{t=1}^{T}$. Then, the empirical cumulative distribution of $||\boldsymbol{S}_0(\boldsymbol{\theta}))|| - ||\boldsymbol{S}_1(\boldsymbol{\theta})||$ are drawn using 100,000 simulations of $||\boldsymbol{S}_0(\boldsymbol{\theta})||$ and $||\boldsymbol{S}_1(\boldsymbol{\theta})||$.

The cumulative distributions of $||\boldsymbol{S}_0(\boldsymbol{\theta})|| - ||\boldsymbol{S}_1(\boldsymbol{\theta})||$ for the 2 parameter vectors are shown in Figures 3 and 4. From Figure 3, the probability that $||\boldsymbol{S}_0(\boldsymbol{\theta}^*)|| - ||\boldsymbol{S}_1(\boldsymbol{\theta}^*)|| > 0$ is 0.5. This indicates that the multivariate SPS method can calculate the exact confidence region for every given confidence probability. From Figure 4, on the other hand, $||\boldsymbol{S}_0(0.95\boldsymbol{\theta}^*)|| - ||\boldsymbol{S}_1(0.95\boldsymbol{\theta}^*)||$ is larger than 0 in all the trials. Therefore, when $||\boldsymbol{\theta} - \boldsymbol{\theta}^*||$ is large, $Rank(\boldsymbol{\theta})$ is likely to be large, that is, $\boldsymbol{\theta}$ is determined to be excluded from the confidence region by multivariate SPS.

Conclusions and future work

In this paper, SPS, which was proposed in (Csaji et al., 2015), (Csaji and Weyer, 2015), and (Volpe et al., 2015), was extended so that it can be used for multivariate processes, especially multivariate ARX processes. The multivariate SPS method exploits the linear regression form where the output vector is expressed as the sum of the noise innovation vector and the product between the regressor matrix and the parameter vector to define the reference sum and the sign-perturbed sums. It was theoretically proved that multivariate SPS provides the exact confidence region with a given probability. In addition, the validity of the extended SPS method was confirmed through a numerical example of a 2-input, 2-output, first-order ARX process controlled by PI controllers. As a result, it was shown that the extended SPS method can calculate the exact confidence region with a given confidence probability; the absolute error between the empirical and given probabilities was at most 0.14%. Moreover, it was confirmed that the parameter vector far from the true parameter vector is excluded from the confidence region.

SPS explores the complete confidence region by calculating the value of the indicator function for a lot of parameter vectors. Hence, when the simple grid search is used for searching the parameter vectors included in the confidence region, the computational burden increases exponentially against the order of the parameter vector. This computation problem is more serious in multivariate SPS than in SPS for single-input, single-output processes, because of the large order of the parameter vector in the former. Practically, the outer approximation method which calculates approximately the confidence region within polynomial time can avoid the curse of dimensionality (Csaji et al., 2015; Volpe et al., 2015). However, the method to determine the confidence region accurately in a short time is still open. Therefore, an efficient method for SPS to search the complete confidence region must be provided to use the extended SPS method, which will be one of our future works.

Acknowledgement

This work was supported by JST SPRING, Grant Number JPMJSP2110 and JSPS KAKENHI, Grant Number JP22K04816. In addition, M. O. was supported by a graduate exchange fellowship from JGP, Kyoto University.

References

Bazanella, A. S., M. Gevers, and L. Mišković (2010).

Closed-loop Identification of MIMO Systems: A New Look at Identifiability and Experiment Design. *European Journal of Control 16*(3), 228–239.

Campi, M. C. and E. Weyer (2005). Guaranteed Non-asymptotic Confidence Regions in System Identification. *Automatica 41*(10), 1751–1764.

Care, A., B. C. Csaji, M. C. Campi, and E. Weyer (2018). Finite-sample System Identification: An Overview and a New Correlation Method. *IEEE Control Systems Letters 2*(1), 61–66.

Csaji, B. C., M. C. Campi, and E. Weyer (2015). Sign-perturbed Sums: A New System Identification Approach for Constructing Exact Non-asymptotic Confidence Regions in Linear Regression Models. *IEEE Transactions on Signal Processing 63*(1), 169–181.

Csaji, B. C. and E. Weyer (2015). Closed-loop Applicability of the Sign-perturbed Sums method. *54th IEEE Conference on Decision and Control (CDC)*, 1441–1446.

Darby, M. L. and M. Nikolaou (2012). MPC: Current Practice and Challenges. *Control Engineering Practice 20*(4), 328–342.

Forssell, U. and L. Ljung (1999). Closed-loop Identification Revisited. *Automatica 35*(7), 1215–1241.

Ljung, L. (1999). *System Identification: Theory for the User Second Edition*.

Shardt, Y. A. W. and B. Huang (2011a). Closed-loop Identification Condition for ARMAX Models Using Routine Operating Data. *Automatica 47*(7), 1534–1537.

Shardt, Y. A. W. and B. Huang (2011b). Closed-loop Identification with Routine Operating Data: Effect of Time Delay and Sampling Time. *Journal of Process Control 21*(7), 997–1010.

Soderstrom, T., L. Ljung, and I. Gustavsson (1976). Identifiability Conditions for Linear Multivariable Systems Operating Under Feedback. *IEEE Transactions on Automatic Control 21*(6), 837–840.

Volpe, V., B. C. Csaji, A. Care, E. Weyer, and M. C. Campi (2015). Sign-Perturbed Sums (SPS) with instrumental variables for the identification of ARX systems. *54th IEEE Conference on Decision and Control (CDC)*, 2115–2120.

Wang, J., T. Chen, and B. Huang (2004). Closed-loop Identification via Output Fast Sampling. *Journal of Process Control 14*(5), 555–570.

Yan, W., C. Du, and C. K. Pang (2015). A General Multirate Approach for Direct Closed-loop Identification to the Nyquist Frequency and Beyond. *Automatica 53*, 164–170.

Proof of Theorem 2

SPS provides the exact confidence region with probability $1-\tilde{R}/R$ for $\forall R\in\{2,3,\cdots\}$ and $\forall\tilde{R}\in\{1,\cdots,R\}$, if and only if $||\boldsymbol{S}_0(\boldsymbol{\theta}^*)||$ is the ρ'-th smallest entry of $\{||\boldsymbol{S}_\rho(\boldsymbol{\theta}^*)||\}_{\rho=0}^{R-1}$ according to $\prec_\pi$ with probability $1/R$ for $\forall\rho'\in\{1,\cdots,R\}$. The latter is easily derived if it is proved that $\{||\boldsymbol{S}_\rho(\boldsymbol{\theta}^*)||\}_{\rho=0}^{R-1}$ is *uniformly ordered* w.r.t. $\prec_\pi$. The main objective of the following is to prove this.

From assumption A.5, it follows that the realization of the external signal vector, $\boldsymbol{u}(t)$ in the case of open-loop systems or $\boldsymbol{y}_{\rm set}(t)$ in the case of closed-loop systems, is fixed. Define $\{\xi_{\rho,n}(t)\}_{t=1}^T$ and $\{\boldsymbol{\Xi}_\rho(t)\}_{t=1}^T$ as

$$\xi_{\rho,n}(t)=\begin{cases}1, & \rho=0,\\ \alpha_{\rho,n}(t), & \text{otherwise},\end{cases}\tag{39}$$

$$\boldsymbol{\Xi}_\rho(t)=\begin{bmatrix}\xi_{\rho,1}(t) & & 0\\ & \ddots & \\ 0 & & \xi_{\rho,N}(t)\end{bmatrix}\in\mathbb{R}^{N\times N}.\tag{40}$$

Then, from Eq. (18), the *reference sum* and *sign-pertubed sums* at $\boldsymbol{\theta}^*$ is expressed as

$$\boldsymbol{S}_\rho(\boldsymbol{\theta}^*)=\boldsymbol{R}_\rho^{-\frac{1}{2}}\frac{1}{T}\sum_{t=1}^T\boldsymbol{\Phi}_\rho(t)\boldsymbol{\Xi}_\rho(t)\boldsymbol{e}(t).\tag{41}$$

Substituting Eqs. (19) and (26) to Eq. (41) gives

$$\boldsymbol{S}_\rho(\boldsymbol{\theta}^*)=\left[\boldsymbol{S}_{\rho,1}^\top(\boldsymbol{\theta}^*)\cdots\boldsymbol{S}_{\rho,N}^\top(\boldsymbol{\theta}^*)\right]^\top,\tag{42}$$

$$\boldsymbol{S}_{\rho,n}(\boldsymbol{\theta}^*)=\boldsymbol{R}_{\rho,n}^{-\frac{1}{2}}\frac{1}{T}\sum_{t=1}^T\boldsymbol{\phi}_{\rho,n}(t)\xi_{\rho,n}(t)e_n(t).\tag{43}$$

Since the external signal vector is fixed, $||\boldsymbol{S}_{\rho,n}(\boldsymbol{\theta}^*)||^2$ is a function of $\{\xi_{\rho,n}(t)e_n(t)\}_{t=1}^T$. Hence, from Eq. (42),

$$||\boldsymbol{S}_\rho(\boldsymbol{\theta}^*)||^2=\sum_{n=1}^N g_n(\xi_{\rho,n}(1)e_n(1),\cdots,\xi_{\rho,n}(T)e_n(T)),\tag{44}$$

where $g_n(\cdot)$ is the measurable function whose output corresponds to $||\boldsymbol{S}_{\rho,n}(\cdot)||^2$.

Here, $e_n(t)$ is divided into the absolute value $v_n(t)=|e_n(t)|$ and the sign $\sigma_n=\text{sign}(e_n(t))$, where $\text{sign}(\cdot)$ is a function which returns the sign of the input. Let $\gamma_{\rho,n}(t)=\xi_{\rho,n}(t)\sigma_n(t)$, then $\{\gamma_{\rho,n}(t)\}_{t=1}^T$ is i.i.d. from Lemma 1 in (Csaji et al., 2015), and $||\boldsymbol{S}_\rho(\boldsymbol{\theta}^*)||^2$ is a function of $\{\gamma_{\rho,n}(t)v_n(t)\}_{t=1}^T(n=1,\cdots,N)$ since

$$||\boldsymbol{S}_\rho(\boldsymbol{\theta}^*)||^2=\sum_{n=1}^N g_n(\gamma_{\rho,n}(1)v_n(1),\cdots,\gamma_{\rho,n}(T)v_n(T)).\tag{45}$$

Let $\{v_n(t)\}_{t=1}^T(n=1,\cdots,N)$ be fixed to a realization, and then $\{||\boldsymbol{S}_\rho(\boldsymbol{\theta}^*)||^2\}_{\rho=0}^{R-1}$ is i.i.d. from the fact that the sum of the outputs of measurable functions whose inputs are i.i.d. are also i.i.d. From this, based on Lemma 3 in (Csaji et al., 2015), $\{||\boldsymbol{S}_\rho(\boldsymbol{\theta}^*)||^2\}_{\rho=0}^{R-1}$ is *uniformly ordered* w.r.t. $\prec_\pi$ under the condition where $\{v_n(t)\}_{t=1}^T(n=1,\cdots,N)$ and the external signal vector are realized. Moreover, the same statement holds without fixing any realizations from Lemma 2 in (Csaji et al., 2015) because it is independent of the particular realizations of $\{v_n(t)\}_{t=1}^T(n=1,\cdots,N)$ and the external signal vector. Finally, $\{||\boldsymbol{S}_\rho(\boldsymbol{\theta}^*)||\}_{\rho=0}^{R-1}$ is also *uniformly ordered* with respect to $\prec_\pi$ since

$$\begin{aligned}&||\boldsymbol{S}_{\rho_1}(\boldsymbol{\theta}^*)||\prec_\pi\cdots\prec_\pi||\boldsymbol{S}_{\rho_R}(\boldsymbol{\theta}^*)||\\ \Leftrightarrow\quad&||\boldsymbol{S}_{\rho_1}(\boldsymbol{\theta}^*)||^2\prec_\pi\cdots\prec_\pi||\boldsymbol{S}_{\rho_R}(\boldsymbol{\theta}^*)||^2,\end{aligned}\tag{46}$$

for any permutation $\forall\{\rho_1,\cdots,\rho_R\}$ of $\{0,\cdots,R-1\}$. *Q.E.D.*